DIRECT-DRIVE INERTIAL FUSION RESEARCH AT THE UNIVERSITY OF ROCHESTER'S LABORATORY FOR LASER ENERGETICS: A REVIEW

R.L. McCrory, D.D. Meyerhofer, S.J. Loucks, S. Skupsky, R.E. Bahr, R. Betti, T.R. Boehly, R.S. Craxton, T.J.B. Collins, J.A Delettrez, W.R. Donaldson, R. Epstein, K.A. Fletcher,[1] C. Freeman,[1] J.A. Frenje,[2] V.Yu. Glebov, V.N. Goncharov, D.R. Harding, P.A. Jaanimagi, R.L. Keck, J.H. Kelly, T.J. Kessler, J.D. Kilkenny, J.P. Knauer, C.K. Li,[2] L.D. Lund, J.A. Marozas, P.W. McKenty, F.J. Marshall, S.F.B. Morse, S. Padalino,[1] R.D. Petrasso,[2] P.B. Radha, S.P. Regan, S. Roberts, T.C. Sangster, F.H. Séguin,[2] W. Seka, V.A. Smalyuk, J.M. Soures, C. Stoeckl, K.A. Thorp, B. Yaakobi, and J.D. Zuegel

University of Rochester
Laboratory for Laser Energetics
250 East River Road
Rochester, NY 14623, U.S.A.

[1]State University of New York, Geneseo
Geneseo, New York, U.S.A.

[2]Massachusetts Institute of Technology
Plasma Science and Fusion Center
Cambridge, MA, U.S.A.

ABSTRACT

This paper reviews the status of direct-drive inertial confinement fusion (ICF) research at the University of Rochester's Laboratory for Laser Energetics (LLE). LLE's goal is to demonstrate direct-drive ignition on the National Ignition Facility (NIF) by 2014. Baseline "all-DT" NIF direct-drive ignition target designs have been developed that have a predicted gain of 45 (1-D) at a NIF drive energy of ~1.6 MJ. Significantly higher gains are calculated for targets that include a DT-wicked foam ablator. This paper also reviews the results of both warm fuel and initial cryogenic-fuel spherical target implosion experiments carried out on the OMEGA UV laser. The results of these experiments and design calculations increase confidence that the NIF direct-drive ICF ignition goal will be achieved.

1. INTRODUCTION

The mission of the University of Rochester's (UR's) Laboratory for Laser Energetics (LLE) is to investigate the interaction of intense radiation with matter. In the pursuit of this

Current Trends in International Fusion Research — Proceedings of the Fifth Symposium
Edited by Emilio Panarella and Roger Raman. NRC Research Press, National Research Council of Canada, Ottawa, ON K1A 0R6 Canada, 2008.

mission, LLE's principal focus is the study of direct-drive inertial confinement fusion (ICF) [1]. Direct-drive ICF offers the potential for higher gain and simple cryogenic targets than the indirect-drive approach. As the lead laboratory for this approach within the U.S. Department of Energy (DOE) NNSA ICF Program, LLE explores all aspects of direct-drive ICF (see Fig. 1); its goal is to demonstrate direct-drive ICF ignition on the National Ignition Facility (NIF) by 2014, and possibly significantly before this date.

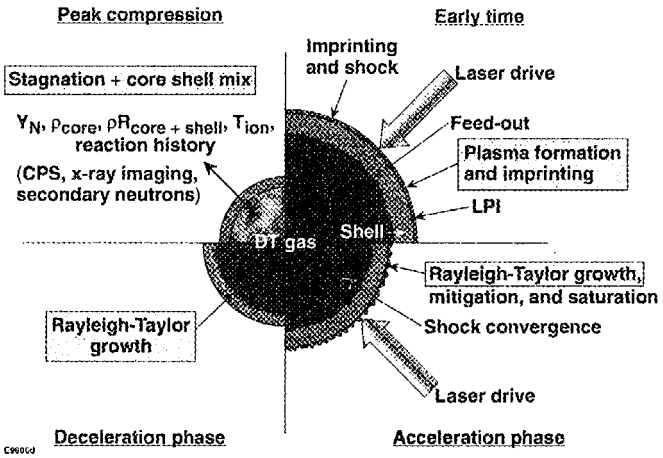

Figure 1. LLE's target physics research program covers all aspects of direct-drive ICF.

LLE's program includes the development of target designs for direct-drive ignition experiments on the NIF; experiments with cryogenic and noncryogenic targets on the 60-beam, 30-kJ OMEGA laser system; diagnostic and target development for OMEGA and NIF; and studies of key aspects of direct-drive ICF physics, including hydrodynamic instabilities, laser imprinting, and laser–plasma interactions.

LLE has made significant progress toward the NIF direct-drive ignition objective.[2,3] Some of this progress is outlined in this paper. The LLE results increase confidence that direct-drive ignition will be demonstrated on the NIF and enhance the prospects for the development of an inertial fusion energy (IFE) power plant.[4]

2. TARGET DESIGNS

The hydrodynamic stability of direct-drive ignition targets depends on the laser irradiation uniformity, capsule ablator, and DT-ice nonuniformities as well as on the implosion adiabat α (the ratio of the internal pressure to the Fermi-degenerate pressure). The higher the adiabat, the more stable the implosion, but the lower the target gain. The baseline LLE NIF direct-drive ignition target design is the $\alpha = 3$, "all-DT" design[5] shown schematically in Fig. 2(a). The baseline design achieves a calculated one-dimensional (1-D) fusion gain of ~45; the gain is reduced to ~30 when two-dimensional (2-D) effects at the anticipated levels of laser and target nonuniformities are included.[5]

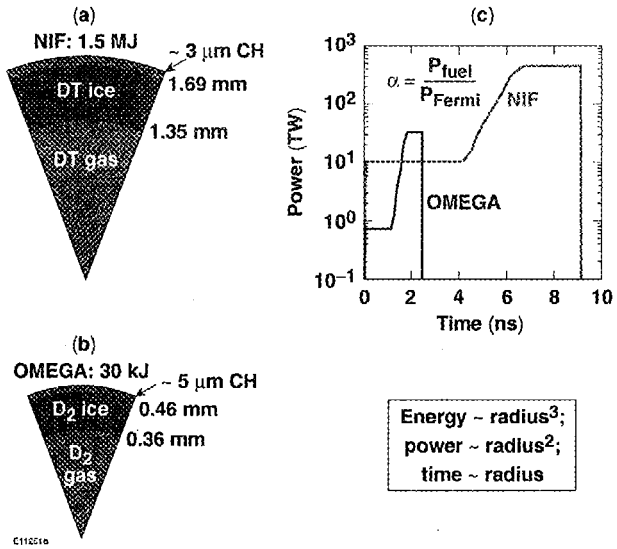

Figure 2. (a) Schematic representation of baseline NIF "all-DT" direct-drive ignition target design; (b) OMEGA (30-kJ) cryogenic target design energy scaled to the NIF design; (c) comparison of NIF and OMEGA baseline ~4 pulse shapes.

Recent progress has also been made on the design of a target comprised of a spherical foam shell wicked with DT [6]. The advantage of this design (see Fig. 3) over the all-DT target is the presence of higher-Z material (CH) in the laser deposition region. The higher-Z material increases the energy absorbed by the capsule. For NIF capsules, the absorption increases by ~40% (from ~60% absorption in DT to ~90% with the wetted foam). In some previous target designs [7] with foam ablators, the foams were doped with high-Z materials and used to radiatively preheat the ablator to mitigate the Rayleigh–Taylor instability.

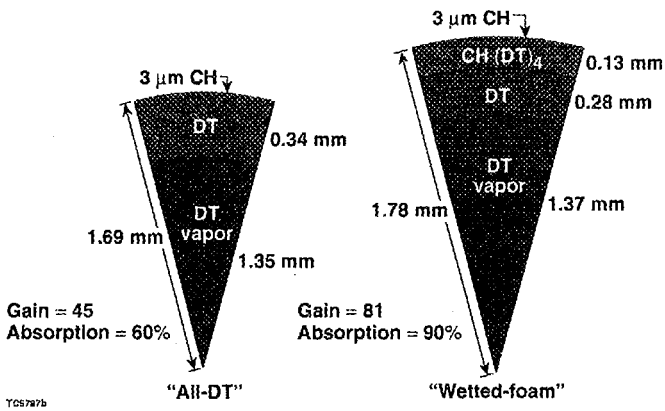

Figure 3. Schematic representation of baseline NIF direct-drive "all-DT" target compared to the "wetted-foam" target design. The baseline design achieves an absorption of ~60% and a 1-D gain of ~45, whereas the "wetted-foam" target absorbs ~90% of the laser energy and achieves a calculated 1-D gain of ~81.

The "wetted-foam" design is more stable than the all-DT design during the acceleration phase of the implosion. Detailed 2-D hydrodynamic simulations are in progress. The wetted-foam capsule design will be tested on the OMEGA laser.

LLE is investigating the use of adiabat shaping to reduce the RT growth rate [8]. One such idea proposed in the past is based on radiation preheat.[9] The present work is aimed at adiabat shaping by launching a shock whose strength decreases as the shock travels through the shell. This creates an adiabat gradient directed toward the ablation front. The time variation in the shock strength is imposed by using an intensity picket in front of the main-drive pulse. The principle underlying this concept is shown schematically in Fig. 4. In this design the main fuel layer is maintained at a low adiabat while the ablation surface has a much higher adiabat, reducing hydrodynamic instability growth rates.

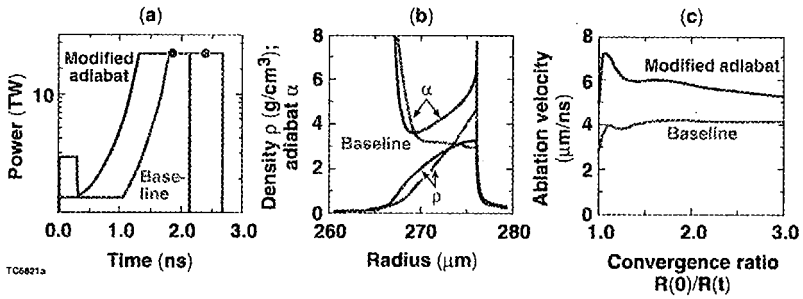

Figure 4. The concept of adiabat shaping via the use of a picket prepulse. (a) Laser pulse shapes of a baseline pulse (red or dashed) compared to a modified adiabat pulse with picket prepulse (blue or solid). (b) Density and adiabat profiles for a typical shell implosion without adiabat shaping (baseline–red or dashed) compared to those with a picket pulse (blue or solid). The exterior surface of the shell is at a higher adiabat with the picket pulse than with the baseline pulse shape. The interior of the shell is not significantly different for these two conditions. (c) Ablation velocities compared for the two cases. The higher ablation velocity attained with the picket pulse shape reduces the RT growth.

LLE's calculations show that a short, intense pulse ahead of the main-drive pulse (picket pulse) reduces the laser imprint as well as the RT growth rate at the ablation surface of the imploding target. As shown in Fig. 5 for an OMEGA simulation, there is a significant reduction in shell nonuniformity when a picket pulse is used compared to the standard design. Simulations of NIF direct-drive cryogenic targets show similar behavior.

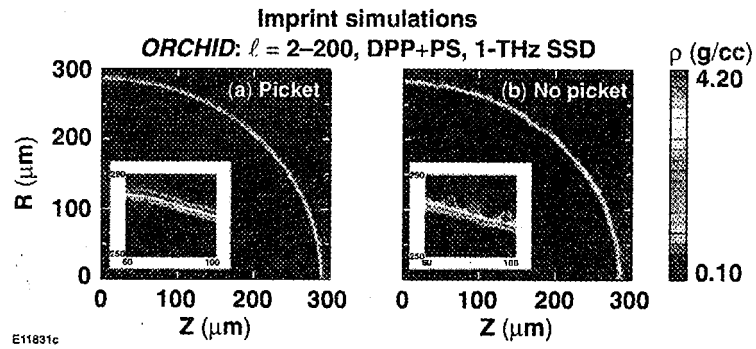

Figure 5. Isodensity contours from *ORCHID* 2-D code simulations of the (a) picket and (b) standard OMEGA α = designs. At the time shown on these plots, the shell has moved ~100 μm in both cases.

3. TARGET EXPERIMENTS AND DIAGNOSTICS

OMEGA is currently the world's most powerful laser facility[10,11] and has unique capabilities to conduct direct-drive implosion experiments. It is a 60-beam UV laser system with an energy capability of 30 kJ on target; variable pulse shapes; 1-THz, 2-D, smoothing by spectral dispersion (SSD),[12] and polarization smoothing.[13]

OMEGA implosion experiments use a comprehensive suite of target diagnostics (including core, shell, and mix diagnostics) to test and validate the 1-D and 2-D target design predictions.[2] The primary fuel core diagnostics deployed on these experiments are illustrated schematically in Fig. 6. In general, charged-particle spectroscopy[14] is used to determine shell and fuel areal densities via measurements of yield and spectra of knock-on deuterons, tritons, and protons in DT-filled capsule implosions and secondary protons in DD-filled capsules.[15] Secondary neutron spectroscopy is used to assess the fuel areal density in DD-filled capsules [16]. Time-resolved x-ray spectroscopy measures the electron density and temperature and is used to infer the fuel–shell mix ratio in Ar-doped, DD-filled capsule implosions.[17]

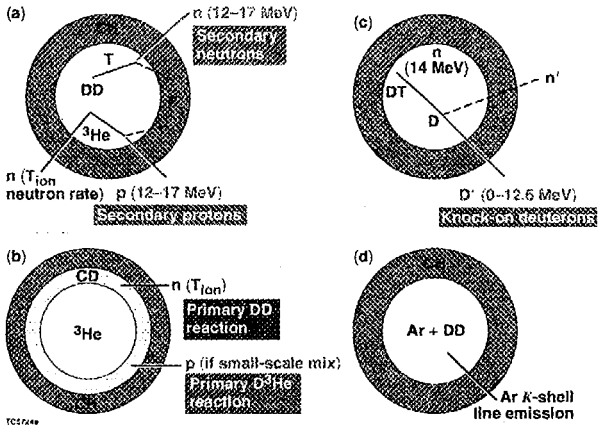

Figure 6. Different types of spherical capsules are used on OMEGA so that complementary diagnostics may be used to characterize hydrodynamically similar implosions. (a) DD-filled shell implosions are diagnosed with secondary neutron and secondary proton spectroscopy; (b) fuel–shell mix is estimated by using thin CD layers placed close to the core gas in ^{3}He-filled CH shell implosions; (c) knock-on particle measurements on made on DT-filled shells, and (d) time-resolved Ar-line and continuum x-ray emission spectroscopy are used to measure the electron density and temperature of Ar-doped DD-filled CH shells.

A series of gas-filled CH shell implosions were carried out on OMEGA driven with an ~23-kJ, 1-ns square pulse and full beam smoothing (1-THz SSD and PS).[2] The ~940-μm-diameter targets had 18- to 24-μm wall thickness and were filled with fuel pressures of 3 and 15 atm D_2 with corresponding predicted (from 1-D hydrodynamic simulations) convergence ratios of ~35 and 14, respectively. The results of these experiments are summarized in Fig. 7. It is evident from this data that the OMEGA laser system provides highly reproducible implosions. In particular, the implosions of the 15-atm-filled, 20-mm-thick shells were taken over a period of two months and show an ~17% standard deviation in the ratio of actual neutron yield over predicted 1-D yield (YOC). The most-stable implosions in this series (24-μm-thick shells with 15-atm fills) have YOC's ~40%. Fuel and shell areal density measurements taken during these experiments along with temporally resolved measurements

of the neutron yield point to shell–fuel mix as the principal reason for the degradation of the measured neutron yield [18].

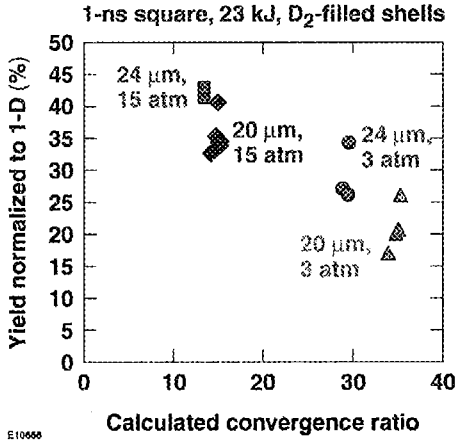

Figure 7. Ratio of the measured to calculated primary neutron yield (YOC) for D_2-filled CH capsule implosions as a function of calculated convergence ratio for 1-THz SSD and PS (from Ref. [2]).

An experiment was carried out to investigate fuel–shell mix and implosion performance in warm-gas implosions as illustrated in Fig. 8. The capsules for this experiment were filled with pure ^{3}He gas, and two different shell configurations were used. The plastic shells had a 1-μm deuterated plastic (CD) layer either placed at the fuel–shell interface or offset from the interface by 1 μm. No primary proton yield is expected for a perfect 1-D implosion in either case. Proton yields are a direct signature of fuel–shell mix. The typical capsule with an offset layer produced a yield ~6 times lower than that with zero offset (see Fig. 8). This proton yield reduction indicates that less CD material was mixed into the fuel because of the finite offset.

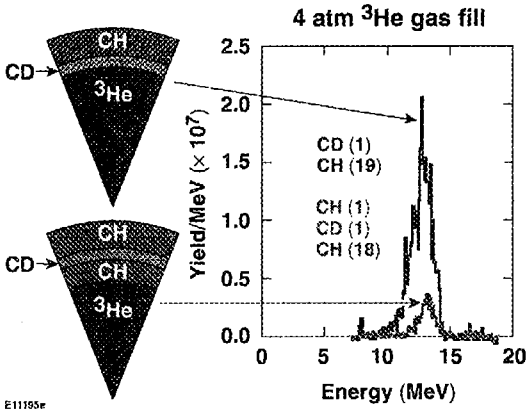

Figure 8. The configuration of two different capsules filled with 4 atm of pure ^{3}He gas, and measured spectra of primary D^{3}He protons from the OMEGA implosions of these capsules. 1-D simulations of the implosion of these capsules predict nearly zero primary proton yield for both targets.

The quantification of the amount of shell mix and its atomic scale were demonstrated on OMEGA experiments using the combination of x-ray spectroscopy, charged-particle spectroscopy, and x-ray imaging.[17] This experiment used plastic shells (CH) filled with

deuterium doped with small amounts of Ar. The emissivity-averaged core electron temperature (T_e) and density (n_e) were inferred from the measured time-dependent Ar *K*-shell spectral line shapes and produced data such as those shown in Fig. 9.

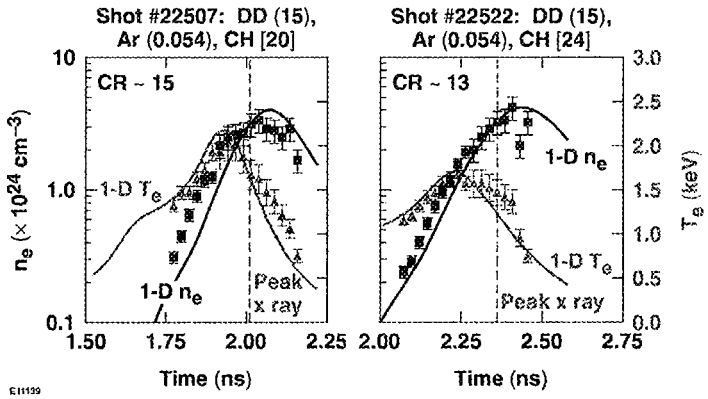

Figure 9. Direct time-resolved measurements of the electron density (n_e) and temperature (T_e) of a 0.9-mm-diam CH shell filled with 15 atm of deuterium and a partial pressure of 0.054 atm of Ar. The capsule for shot 22057 was 20 m thick while that for shot 22522 was 24 m thick (from Ref. [17]).

A detailed analysis of data from shot 22057 indicates that the composition of the mantle of fuel surrounding the central hot spot of the compressed core consists of ~50% deuterium and ~50% CH. The inferred total fuel pressure (electrons and ions) at the time of peak neutron burn is estimate at ~11 Gbar. Such implosions have produced a fusion figure of merit (product of density, temperature, and confinement time) of ~7×10^{20} keV s m^3—comparable to that obtained on the highest-performance Tokamak magnetic fusion experiments.[19]

Cryogenic D_2 capsule implosion experiments have been conducted on OMEGA.[20,21] The experiments are designed to measure the sensitivity of the direct-drive implosion performance to key parameters such as the target ice roughness, the capsule adiabat, laser energy deposition uniformity, and target positioning accuracy. These experiments are being conducted using a capsule configuration consisting of a thin shell (typically ~5 μm thick) of GDP or CD [22]. The shells are permeation filled with approximately 1000 atm of D_2 and then cooled to the triple point (18.73 K) to produce an ice-layer thickness of ~100 μm. Initial cryogenic target experiments (see Fig. 10) with such targets have produced YOC of up to ~50% to 100% and areal densities ~80% to 100% of 1-D predictions for high-adiabat pulse shapes ($\alpha \sim 25$). Lower-adiabat ($\alpha \sim 5$) pulse shape target implosions (see Fig. 11) have achieved YOC of ~11% and 2-D calculated yield approximately equal to the measured yield.

The recent cryogenic target experiments on OMEGA have pointed out the need for high-precision target alignment. The cryogenic targets are mounted using a spider silk web attached to a "C"-shaped mount [23]. Although, the alignment accuracy of the target positioning and viewing system has been measured to be better than 5 μm for noncryogenic capsules, it was found that the rapid withdrawal of the cooling shroud prior to the shot could under certain conditions create large-amplitude vibrations that caused the target to be offset from its nominal position at the center of the target chamber at shot time.

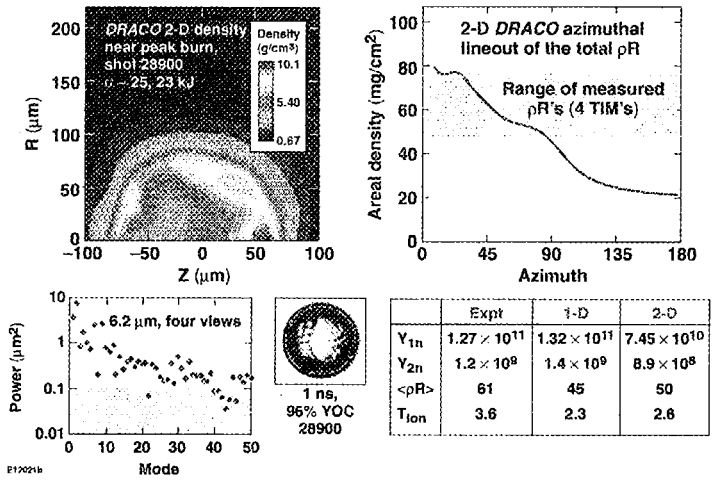

Figure 10. Summary of the results of a high-adiabat cryogenic capsule implosion. Upper left—density contour plot from *DRACO* 2-D hydrodynamics code simulation of an $\alpha \sim 25$ implosion (shot 28900); upper right—*DRACO*-predicted angular distribution of capsule areal density (red solid line) compared to the range of measured areal density (measured using four range filter charged-particle spectrometers placed at various angles); lower left—measured ℓ-mode ice-surface uniformity based on four views; lower center—shadowgraph of target; lower right—table summarizing experimental results compared to 1-D and 2-D simulations. This target achieved ~96% of the predicted neutron yield and exceeded the predicted 1-D capsule areal density.

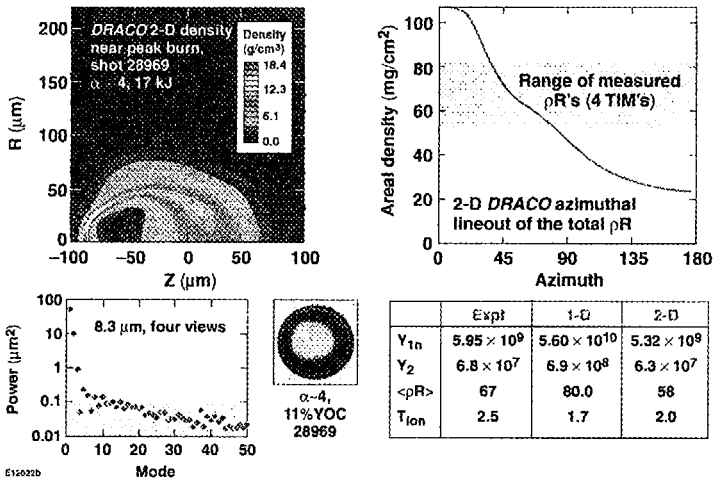

Figure 11. Summary of the results of an OMEGA low-adiabat cryogenic capsule implosion. Upper left—density contour plot from *DRACO* 2-D hydrodynamics code simulation of an $\alpha \sim 4$ implosion (shot 28969); upper right—*DRACO*-predicted angular distribution of capsule areal density (red solid line) compared to the range of measured areal density (measured using four range filter charged-particle spectrometers placed at various angles); lower left—measured ℓ-mode ice-surface uniformity based on four views; lower center—shadowgraph of target; lower right—table summarizing experimental results compared to 1-D and 2-D simulations. This target achieved ~11% of the predicted neutron yield and ~84% of the predicted 1-D capsule areal density. The measured neutron yield and areal density agree well with the 2-D *DRACO* prediction.

Figure 12 shows the results of an $\alpha \sim 25$ cryogenic target implosion where the target was offset by ~85 μm from its nominal position (shot 25477) to that of an $\alpha \sim 25$ capsule implosion with an offset of only 14±7 μm (shot 28900).

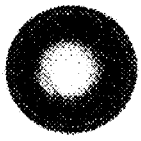

Shot 26477			Shot 28900	
Drive pulse: 1 ns ($\alpha \sim 25$)				
	Experimental	Clean 1-D (%)	Experimental	Clean 1-D (%)
Yield (1n):	3.17×10^{10}	31	1.27×10^{11}	96
Yield (2n):	3.05×10^{8}	32	1.17×10^{9}	84
Yield (2p):	2.67×10^{7}	21	2.03×10^{8}	112
$\langle \rho R \rangle$:	30 mg/cm^2	80	61 mg/cm^2	133
T_{ion}:	2.6 keV	117	3.6 keV	157
Y_{2n}/Y_{1n}:	0.0096	102	0.0092	85
Y_{2p}/Y_{1n}:	0.00084	66	0.0016	114
TCC offset:	85 μm		14±7 μm	

E12016b

Figure 12. A comparison of shots 28900 and 26477 clearly shows that target offset can be an important contributor to reduced performance even for high-adiabat pulse shape shots. Both of these targets were irradiated with an $\alpha \sim 25$ pulse shape, but the target with the larger offset (26477) suffered a yield reduction of ~3× compared to that with the smaller offset (28900).

4. FUTURE DIRECTIONS

Future experiments on OMEGA will be directed toward improved laser uniformity (improved DPP's), improvements in the fabrication of cryogenic capsules, higher-precision target placement, wetted-foam capsules, and picket-fence-pulse-shape capsule implosions.

The successful demonstration of the wetted-foam and picket-pulse concepts on OMEGA would motivate an attempt to achieve direct-drive ignition on the NIF as soon as the NIF symmetry allows. While the NIF is designed "not to preclude" the implementation of direct-drive targets, a changeover from the baseline indirect-drive configuration could be expensive and costly. Laser deposition uniformity calculations indicate that it may be possible to achieve an adequate symmetry for direct-drive targets using the NIF polar direct-drive (PDD) concept (repointing NIF beams in the x-ray drive configuration). An example of a calculated irradiation uniformity distribution based on such a configuration is shown in Fig. 13.

In addition to the conventional direct-drive approach, LLE plans to extend its ICF and high-energy-density physics capabilities by the construction of a new laser facility: OMEGA EP. The new laser will make use of the LLE-developed chirped-pulse-amplifier (CPA) technology[24] to produce peak powers in excess of several petawatts (1 PW = 10^{15} W). With a nominal focused intensity capability of ~6×10^{20} W/cm^2, the new laser will provide new avenues of research as illustrated in Fig. 14. In particular, OMEGA is an ideal facility to perform integrated fast ignition experiments with its cryogenic target capability.[25]

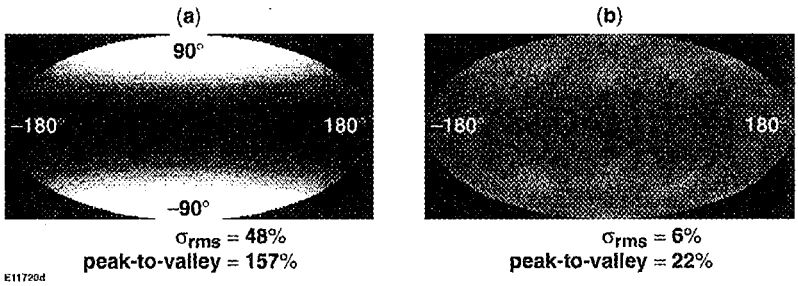

Figure 13. Aitoff projection of laser intensity on a spherical target for the NIF 192-beam indirect-drive beam configuration with (a) beams pointed normal to the spherical target surface and (b) with beams in the polar direct-drive (PDD) configuration. The overall uniformity may be improved further by special phase-plate designs and ice layer/capsule shimming.

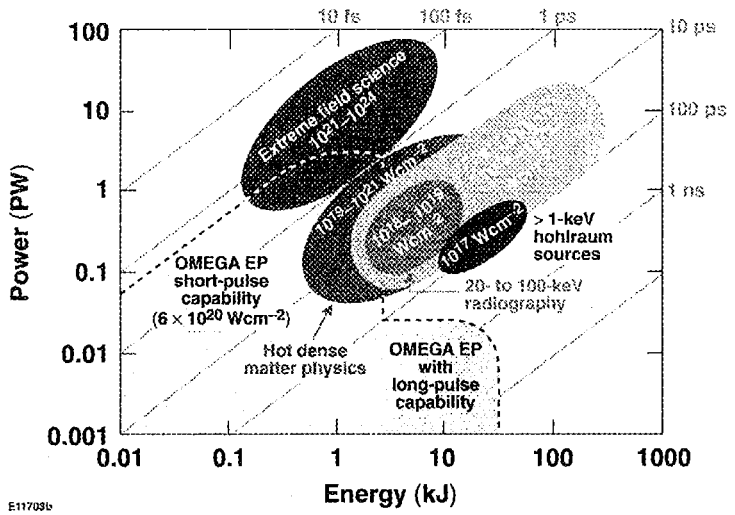

Figure 14. The potential new science areas that may be explored with the OMEGA EP laser.

5. SUMMARY

Significant progress is being made in the comprehensive LLE experimental and theoretical programs on direct-drive ICF. LLE has developed direct-drive ICF capsule designs for the NIF facility with moderate gains (1-D gains of ~45, 2-D gains of ~30 at an energy of ~1.6 MJ). Recent advances in target designs point to even-higher possible gains and more-robust target designs by using wetted-foam capsules and adiabat shaping using picket-pulse laser pulse shapes. High-performance cryogenic capsule implosion experiments are under way using an array of target diagnostics. Exploratory work is also under way to determine whether the NIF indirect-drive beam configuration can be used without substantive changes to carry out high-performance direct-drive experiments. Finally, LLE is in the design stage of a new high-power laser facility (OMEGA EP), which will have multi-PW peak power capability and will be used for a large variety of ICF and high-energy-density physics experiments.

ACKNOWLEDGMENT

This work was supported by the U.S. Department of Energy (DOE) Office of Inertial Confinement Fusion under Cooperative Agreement No. DE-FC03-92SF19460, the University of Rochester, and the New York State Energy Research and Development Authority. The support of the DOE does not constitute an endorsement by the DOE of the views expressed in this article.

REFERENCES

1. J. Nuckolls *et al.*, Nature **239**, 139 (1972).
2. D.D. Meyerhofer *et al.*, Phys. Plasmas **8**, 2251 (2001).
3. R.L. McCrory *et al.*, Nucl. Fusion **41**, 1413 (2001).
4. J. D. Sethian *et al.*, "Fusion Energy with Lasers, Direct-Drive Targets, and Dry Wall Chambers," submitted to Nucl. Fusion (2003).
5. P.W. McKenty *et al.*, Phys. Plasmas **8**, 2315 (2001).
6. R.L. McCrory *et al.*, "Progress in Direct-Drive Inertial Confinement Fusion Research at the Laboratory for Laser Energetics," to be published in the *Proceedings of the 19th IAEA Fusion Energy Conference* and Nuclear Fusion.
7. D.G. Colombant *et al.*, Phys. Plasmas **7**, 2046 (2000).
8. Laboratory for Laser Energetics LLE Review **93**, 18, NTIS document No. DOE/SF/19460-478 (2002). Copies may be obtained from the National Technical Information Service, Springfield, VA 22161.
9. S.E. Bodner *et al.*, Phys. Plasmas **5**, 1901 (1998).
10. J.M. Soures *et al.*, Phys. Plasmas **3**, 2108 (1996).
11. T.R. Boehly *et al.*, Opt. Commun. **133**, 495 (1997).
12. S. Skupsky *et al.*, J. Appl. Phys. **66**, 3456 (1989).
13. T.R. Boehly *et al.*, J. Appl. Phys. **85**, 3444 (1999).
14. F.H. Séguin *et al.*, Rev. Sci. Instrum. **74**, 975 (2003), and references therein.
15. C.K. Li *et al.*, Phys. Plasmas **8**, 4902 (2001), and references therein.
16. F.H. Séguin *et al.*, Phys. Plasmas **9**, 2725 (2002), and references therein.
17. S.P. Regan *et al.*, Phys. Rev. Lett. **89**, 085003 (2002), and references therein.
18. P.B. Radha *et al.*, Phys. Plasmas **9**, 2208 (2002).
19. R.J. Hawryluk *et al.*, Phys. Plasmas **5**, 1577 (1998).
20. C. Stoeckl *et al.*, Phys. Plasmas **9**, 2195 (2002).
21. C. Sangster *et al.*, Phys. Plasmas **10**, 1937 (2003).
22. A. Nikroo *et al.*, Fusion Sci. Technol. **41**, 214 (2002).
23. Laboratory for Laser Energetics LLE Review **81**, 21, NTIS document No. DOE/SF/19460-335 (1999). Copies may be obtained from the National Technical Information Service, Springfield, VA 22161.
24. D. Strickland and G. Mourou, Opt. Commun. **56**, 219 (1985).
25. M. Tabak *et al.*, Phys. Plasmas **1**, 1626 (1994).